International Journal on Interactive Design and Manufacturing (IJIDeM)
https://doi.org/10.1007/s12008-023-01268-x

ORIGINAL PAPER

Evaluation of performance of vibration signatures for condition monitoring of worm gearbox by using ANN

Raghavendra R. Barshikar[1] · **Prasad R. Baviskar**[2]

Received: 7 November 2022 / Accepted: 22 February 2023

Abstract
The worm wheel is the critical element and is vulnerable to failure due to fault occurring on it that leads to downtime hampering productivity. The condition monitoring can predict deteriorating health due to the fault. This work presents the experimental investigation of the worm gearbox carried out by the design of experiments (DOE) that utilizes amplitudes of denoised vibration signatures. During the experiments, trials are designed by the response surface method Box-Behnken DOE method. The cases considered for a single fault are (a) healthy gearbox (b) defective bearing inner race (c) defective outer race (d) defective worm wheel followed by cases comprising of a combination of two faults (e) fault on bearing inner and outer race (f) faulty worm wheel and bearing inner race (g) defective worm wheel and bearing outer race (h) fault on all three was acquired. The statistical parameters extracted from the acquired vibration signatures were used as input to train the ANN model and the performance is evaluated. The results show that the worm wheel is predominant for the fault over the other entities. ANN model predicts fault with an accuracy of 92.9%. Research outcomes envisage that the methodology used has good solidity to improve the performance.

Keywords Worm wheel · Fault · Condition monitoring · Vibration signature · DOE · ANN

1 Introduction

Nowadays condition monitoring plays a vital role in all industries such as chemical, power plants, pharmaceutical, and automobile industries. Correct fault identification, analysis, classification, and severity of fault are vital subjects in the predictive maintenance field. Different predictive maintenance methods like thermal analysis, acoustic analysis, motor current signature analysis, and vibration analysis have been used for fault analysis of gearboxes [1–3]. Out of these methods, vibration analysis is a more popular method for fault identification of gearbox. Predictive maintenance or condition-based maintenance of the gearbox increases efficiency, reliability, safety and productivity, lowers the maintenance cost, and sudden stoppage of the machine [4]. Limited research has been carried out on fault diagnosis of combined faults present in gearboxes by using vibration analysis. The gearbox consists of different components viz shafts, gears, bearings, casing, keys, and couplings. Among these components, gear and bearing are critical components and the nature of the vibration signature for fault present in multiple components of a gearbox is different from the vibration signature of fault present in individual components of the gearbox [5]. In condition monitoring of rotating machinery, extracted vibration signatures from the accelerometer sensors are contaminated by background noise, electromagnetic interference, and vibrations originating from other components of the machine. Hence, the initial task of fault analysis is to separate the actual component vibration signal from the contaminated signal. The denoising method plays a vital role to separate gear and bearing vibration signatures from contaminated vibration signatures [6]. Different denoising algorithms were employed such as improved median filter and wavelet packet [7] synchronous cumulative average noise reduction (SCA) and the denoised signals to separate with the improved fast independent component analysis (FastICA) algorithm [8] gaussian mixture model and quantum-inspired

✉ Raghavendra R. Barshikar
raghavendrabarshikar@gmail.com

Prasad R. Baviskar
prasadbaviskar@gmail.com

[1] Department of Mechanical Engineering, MET's Institute of Engineering, Nashik, SPPU, Pune, India

[2] Department of Mechanical Engineering, Sandip Institute of Technology and Research Centre, Nashik, SPPU, Pune, India

Published online: 22 March 2023

standard deviation and wavelet denoising algorithm [9] to denoised contaminated vibration signature. Mishra et al. [10] presented a wavelet denoising algorithm that is suitable when the shaft frequency is less than 100 Hz.

The different types of faults like tooth breakage, pitting, facture, nicks, scoring, and small holes occur on the worm wheel and bearings of the worm gearbox under varying load and speed. To avoid a sudden breakdown, harm to humans, production, and loss of money, there is a need to early identify and classify faults that occur in the worm gearbox [11]. In a worm gearbox, as the material of the worm wheel is generally softer than that of the worm screw, the worm wheel gear gets pitted or worn out during the sliding process [12]. This failure of the worm wheel gear of the worm gearbox is a matter of concern. A limited number of publications on fault diagnosis of worm gearboxes by using vibration monitoring are published because the acquisition of vibration signature from worm gearbox is a challenging task [13]. Condition monitoring of seeded defects on oil jet sprayed machine worm gears by a combination of acoustic emission and vibration analysis is presented [14]. Elasha et al. [15] presented a research paper that deals with the pitting fault diagnosis of worm gearboxes based on vibration analysis. For the classification of faults and severity of bearing and gear by using advanced methods such as ANN, support vector machine (SVM), and convolutional neural networks (CNN) number of research have been carried out. Umutlu et al. [16] proposed a backpropagation multilayer perceptron ANN technique for the classification of pitting fault severity that occurred on the worm wheel. The results show that the proposed ANN reliably classifies pitting fault severity. Agrawal and Jayaswal [17] implemented two techniques namely ANN and (SVM) to identify and classify rolling element-bearing faults. The implemented ANN and (SVM) techniques achieved 98% and 100% accuracy respectively. Okwudili et al. [18] investigated the identification of different faults on the electric power system transmission line using ANN. Kane and Andhare [19] examined the capability of the ANN technique based on vibration, acoustics, and psychoacoustic statistical parameters to detect and classify healthy, broken teeth, profile teeth error, and cracks at the root of spur gear. Dabrowski et al. [20] studied the effectiveness of the ANN technique in the condition monitoring of industrial machines. Various applications of ANN are classification, severity, diagnosis, speed recognition, image recognition, and random function approximation. Laboratory condition monitoring experiments require systematic plans such as artificial defect size, variation of speed, and load to conduct fault detection experimental trials. In recent research, experimental trials are designed by using technique of design of experiments (DOE), and vibration signature responses are analysed by response surface methodology (RSM) for fault detection in bearing and gear [21–25]. From the available literature, large research has been carried out into the condition monitoring of gearboxes, but most of the research focuses on the condition monitoring of spur and helical gearboxes using vibration analysis as compared to worm gearboxes. Therefore research on combined fault identification of worm gearboxes is a matter of concern.

The current research proposes a backpropagation multilayer perceptron ANN model for combined worm wheel and bearing fault identification. The novelty of the research is that it examines practical conditions i.e. combine worm wheel-bearing fault identification is considered. The faults of different dimensions were created artificially on the worm wheel bearing outer race and inner race and on the worm wheel tooth using a wire cutting machine and file tool respectively. Vibration signatures are captured for these fault conditions using an FFT analyser. Based on the readings, eight statistical parameters are extracted for training the ANN model. ANN model is trained in Matlab to identify faults in the worm wheel and bearing.

2 Methodology and experimentation

2.1 Methodology

The methodology adopted in this research consists of the following steps:

1. Manufacturing of an experimental setup and inducing artificial faults in worm wheel bearing inner race, outer race and worm wheel teeth.
2. Four independent parameters considered are faulty worm wheel bearing outer race, faulty worm wheel bearing inner race, faulty worm wheel and load considered with three levels.
3. Box-Behnken design RSM method is used to perform DOE for experimentation.
4. Calculation of outer race bearing pass frequency (f_{BPOF}), inner race bearing pass frequency (f_{BPIF}) and gear mesh frequency (f_{gm}).
5. Vibration signatures are captured in the frequency domain using an FFT analyser for twenty- seven experiment trials.
6. Eight different statistical parameters extracted from the frequency domain are RMS, crest factor, kurtosis, mean, peak to peak, skewness, sample variance and standard deviation.

2.2 Laboratory experimental test rig

The experiments were performed on the setup as depicted in Fig. 1. The trials were conducted under a constant rotational speed of 2880 r.p.m. provided by a three-phase AC motor

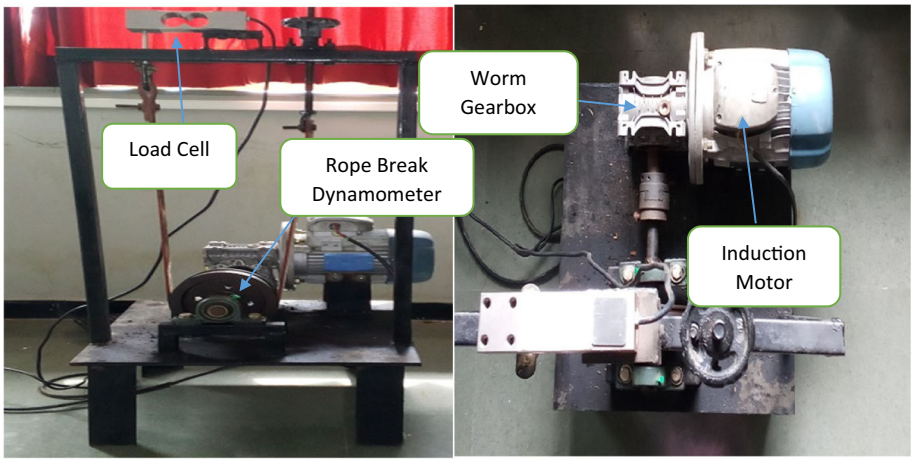

Fig. 1 Photographic view of the experimental setup

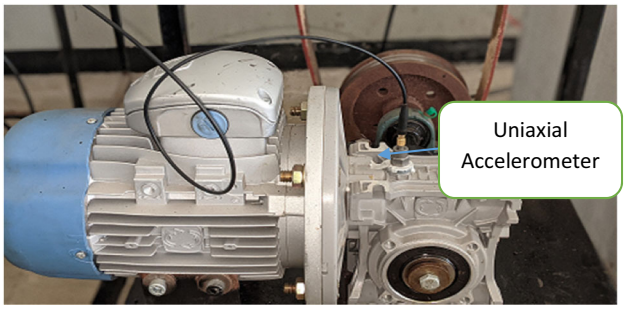

Fig. 2 Mounting of the accelerometer

0.75 kW 2880 rpm. A ribbon blender 1/15 gear ratio worm gearbox is used for experimentation. The worm gearbox consists of a worm of double thread made of case-hardened steel and profile ground. The worm wheel has 30 teeth made of shell-cast ZCuSn12 bronze. The speed of the gearbox is controlled by a variable frequency drive. Figure 2 represent the mounting of accelerometer. The load is applied to the gearbox by the rope break dynamometer and measured by the load cell. In this research, DOE based on the Box-Behnken design RSM method is used to design experimental trials for three levels with four factors as shown in Table 1. The dimensions of faults on bearing inner race, outer race and worm wheel are considered based on available literature. Dhamande and Chaudhari [5], Agrawal and Jayaswal [17] have investigated the fault with the geometry of a circular hole on bearing inner and outer races of varying diameters from 0.1 to 0.8 mm by using an electrical discharge machine. Babu et al. [13] introduced half and full-tooth breakage faults on the worm wheels by using a file tool. Ribbon blender machine work in three phases such as dry phase, semi-wet phase, and wet phase. Therefore load of 10 kg, 15 kg and 20 kg is considered. Figure 3 shows healthy worm wheel and worm wheel bearing. As mentioned in Table 2, twenty-seven different dimensions of artificial faults on the bearing inner race, bearing outer race, and worm wheel teeth are created by using a wire-cutting machine, grinder machine, and file tool. The form of artificial faults is depicted in Fig. 4. Experimental trials were performed to capture vibration signatures in the frequency domain. Table 2 represents twenty-seven experimental trials matrix. In the case of fault identification of the gearbox; the amplitude of vibration signature corresponding to gear mesh frequency, outer race bearing pass frequency, and inner race bearing pass frequency are strong predictors of fault in the gearbox [11, 15].

2.3 The characteristic rotational frequency of worm gearbox

To use vibration effectively and efficiently to monitor the condition of rotating machinery, it is necessary to understand the characteristics of vibration generation. The primary

Table 1 Input parameters with their levels

Symbols for independent parameters	Independent parameters	Minimum level	Middle level	Maximum level
IR	Fault on bearing inner race	0	0.4 mm	0.8 mm
OR	Fault on bearing outer race	0	0.4 mm	0.8 mm
WW	Fault on worm wheel teeth	0	8 mm	16 mm
LOAD	Load applied	10 kg	15 kg	20 kg

(a) **(b)**

Fig. 3 Healthy (**a**) worm wheel (**b**) worm wheel bearing

Table 2 Experimental matrix

Standard order	Experiment run order	Fault type	IR (mm)	OR (mm)	WW (mm)	LOAD (kg)
1	12	FT1	0	0.4	0	15
2	17	FT2	0.4	0	0	15
3	27	FT3	0	0	8	15
4	2	FT4	0.4	0.4	0	10
5	18	FT4	0.4	0.4	0	20
6	9	FT5	0.4	0.8	0	15
7	4	FT6	0.8	0.4	0	15
8	13	FT7	0	0.4	8	10
9	23	FT7	0	0.4	8	20
10	19	FT8	0	0.4	16	15
11	11	FT9	0	0.8	8	15
12	6	FT10	0.4	0	8	10
13	10	FT10	0.4	0	8	20
14	20	FT11	0.4	0	16	15
15	3	FT12	0.8	0	8	15
16	24	FT13	0.4	0.4	16	10
17	7	FT13	0.4	0.4	16	20
18	8	FT14	0.4	0.8	8	10
19	5	FT14	0.4	0.8	8	20
20	21	FT15	0.4	0.4	8	15
21	22	FT15	0.4	0.4	8	15
22	25	FT15	0.4	0.4	8	15
23	16	FT16	0.4	0.8	16	15
24	14	FT17	0.8	0.4	8	10
25	1	FT17	0.8	0.4	8	20
26	15	FT18	0.8	0.4	16	15
27	26	FT19	0.8	0.8	8	15

rotational frequencies associated with rotating elements are considered characteristics of vibration generation that is known as characteristics rotational frequency of rotating elements.

The gear mesh frequency of the worm wheel is calculated by using following the formula,

$$f_{gm} = f_r \times n \tag{1}$$

where, n = number of teeth, f_r = Shaft rotational frequency

If a fault occurs on a tooth surface, a vibration will be induced at this frequency.

Gear mesh frequency at output speed 192 rpm is

$$f_{gm} = \frac{192}{60} \times 30$$

$$f_{gm} = 96Hz$$

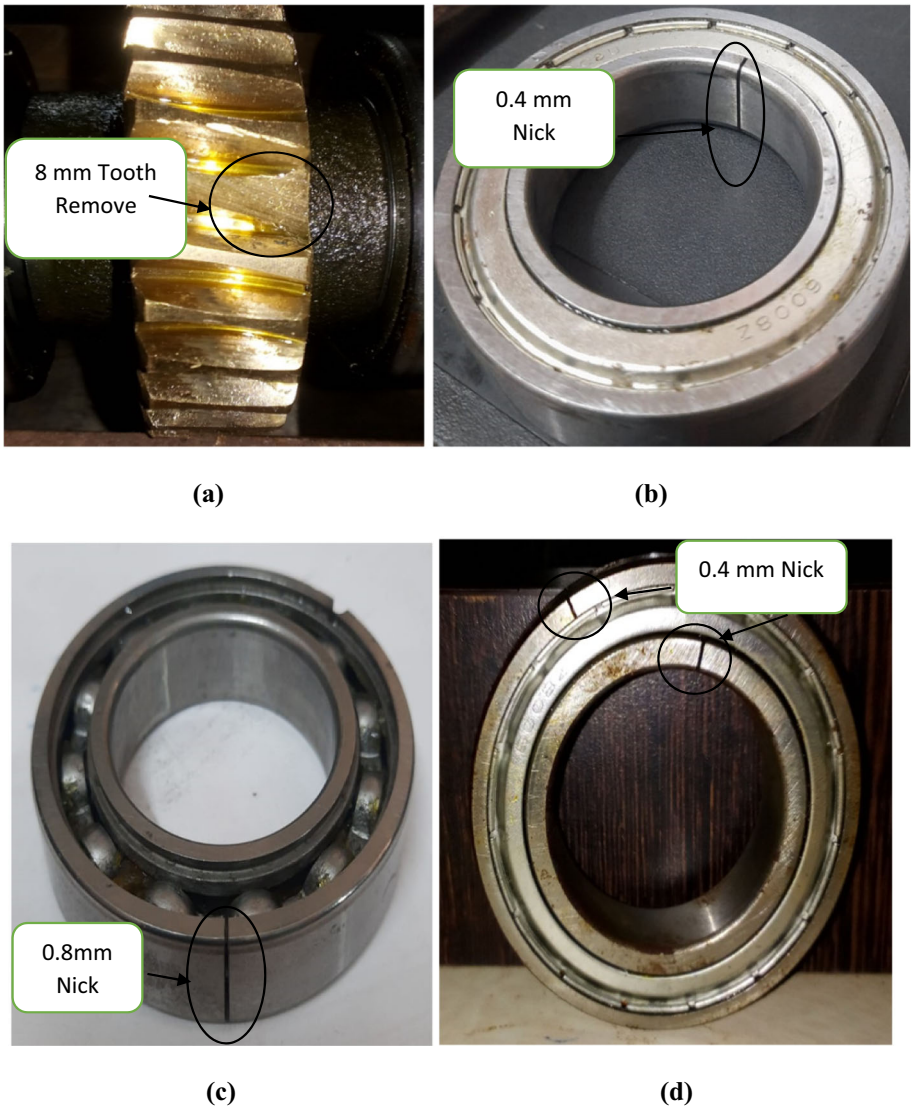

Fig. 4 Artificial faults on (**a**) worm wheel (**b**) bearing inner race (**c**) bearing outer race (**d**) bearing inner and outer race

The characteristic rotational frequency worm wheel bearing is as follows;

$$f_{BPOF} = \frac{f_r}{2} N_b \left(1 - \frac{D_B}{D_C} \cos\theta\right) \tag{2}$$

f_{BPOF} = Outer race bearing pass frequencies

D_C = Cage diameter measured from a ball centre to the opposite ball centre,

D_b = Ball diameter,

N_b = Number of balls,θ = Contact angle between the bearing surfaces.

Outer race elements pass frequencies at an output speed of 192 rpm is

$$f_{BPOF} = \frac{192}{2 \times 60} \times 12 \times \left(1 - \frac{9.4}{54} \times \cos 0\right)$$

$$f_{BPOF} = 15.85Hz$$

$$f_{BPIF} = \frac{f_r}{2} N_b \left(1 + \frac{D_B}{D_C} \cos\theta\right) \tag{3}$$

f_{BPIF} = Inner race elements pass frequencies.

D_C = Cage diameter measured from a ball centre to the opposite ball centre,

D_b = Ball diameter,

N_b = Number of balls,θ = Contact angle between the bearing surfaces.

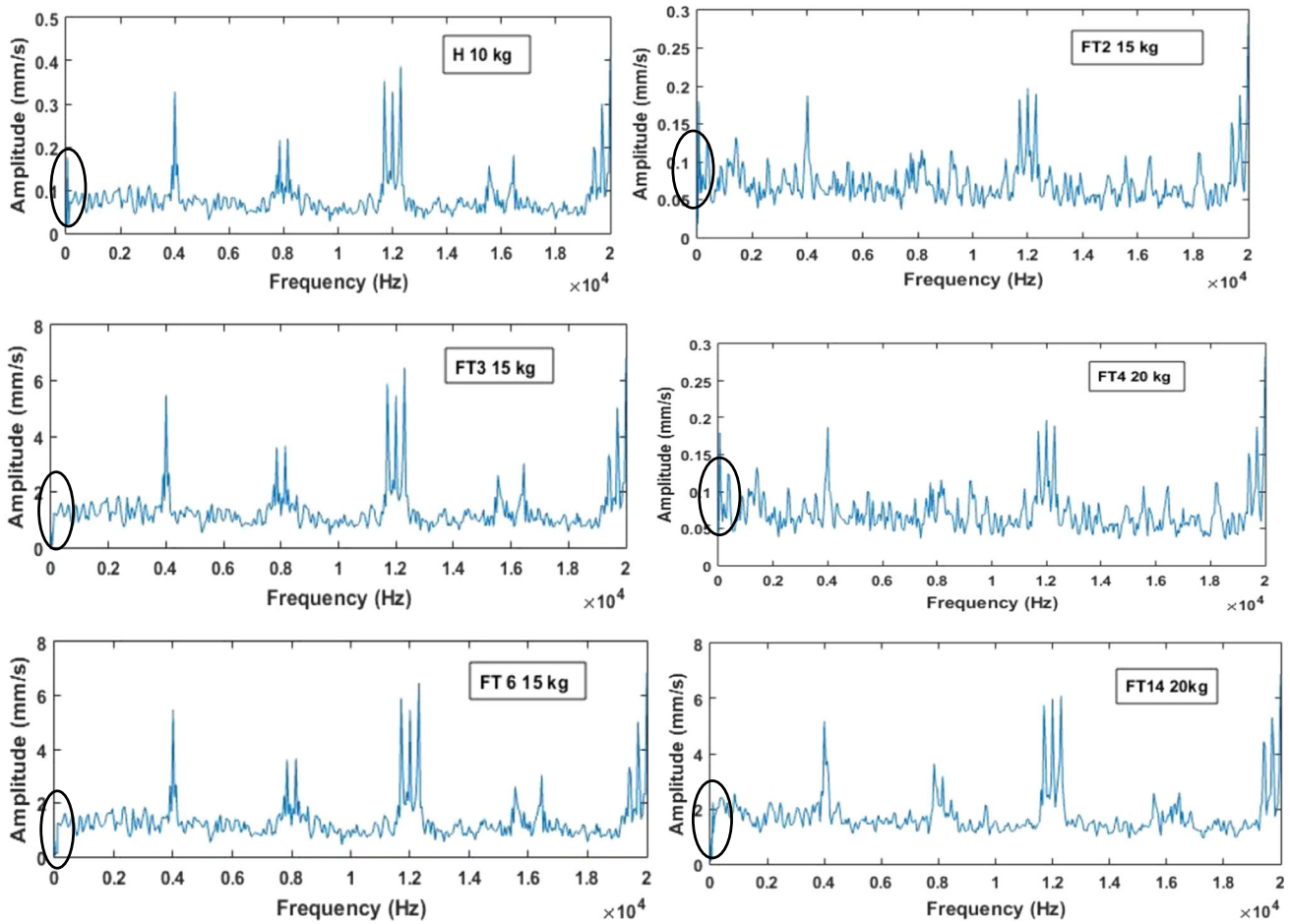

Fig. 5 Contaminated vibration signature of healthy, FT2, FT3, FT4, FT6 and FT14 in the frequency domain

Inner race bearing pass frequencies at an output speed of 192 rpm is

$$f_{BPIF} = \frac{192}{2 \times 60} \times 12 \times \left(1 + \frac{9.4}{54} \times \cos 0\right)$$

$$f_{BPIF} = 22.54Hz$$

2.4 Acquisition of vibration signature by or34 FFT analyser

Vibration signatures for healthy and faulty (twenty-seven faults) conditions are acquired by using an OR34 four-channel FFT analyser and 41A161032 uniaxial accelerometer. Umutlu et al. [16] proved that an accelerometer mounted in a radial direction shows more vibration amplitude than an axial direction. Therefore in this experiment, an accelerometer is mounted in the radial direction as shown in Fig. 2. The experimental test rig is run for 60 s. Each trial repeat for five times to validate the vibration signature [5]. As per the worm gearbox gear ratio, the number of rotations of the worm wheel will be 192. A sampling frequency of 20,000 Hz and sensitivity of 10.03 mv/g are utilized for the experimental trial. Acquired vibration signatures from the accelerometer are recorded on a computer by using NVGate V10.00 software. NVGate V10.00 software is compatible with OR 34 FFT analyser. Initially, captured vibration signatures are contaminated by other component's noise. A few contaminated vibration signatures are shown in Fig. 5. It is difficult to analyse and predict the exact condition of the gearbox by using contaminated vibration signatures.

Therefore, the denoising method is used to reconstruct a vibration signal from a contaminated vibration signal. It aims to remove noise and extract useful information [2]. In these experiments, contaminated vibration signatures are denoised by using the wavelet denoise method. A few denoised vibration signatures are shown in Fig. 6. Wavelet denoise method is based on a thresholding algorithm [25]. The basic aim of the thresholding algorithm is to decompose the signal into two parts namely high frequency signal and low-frequency signal. The wavelet denoise method consists of three steps;

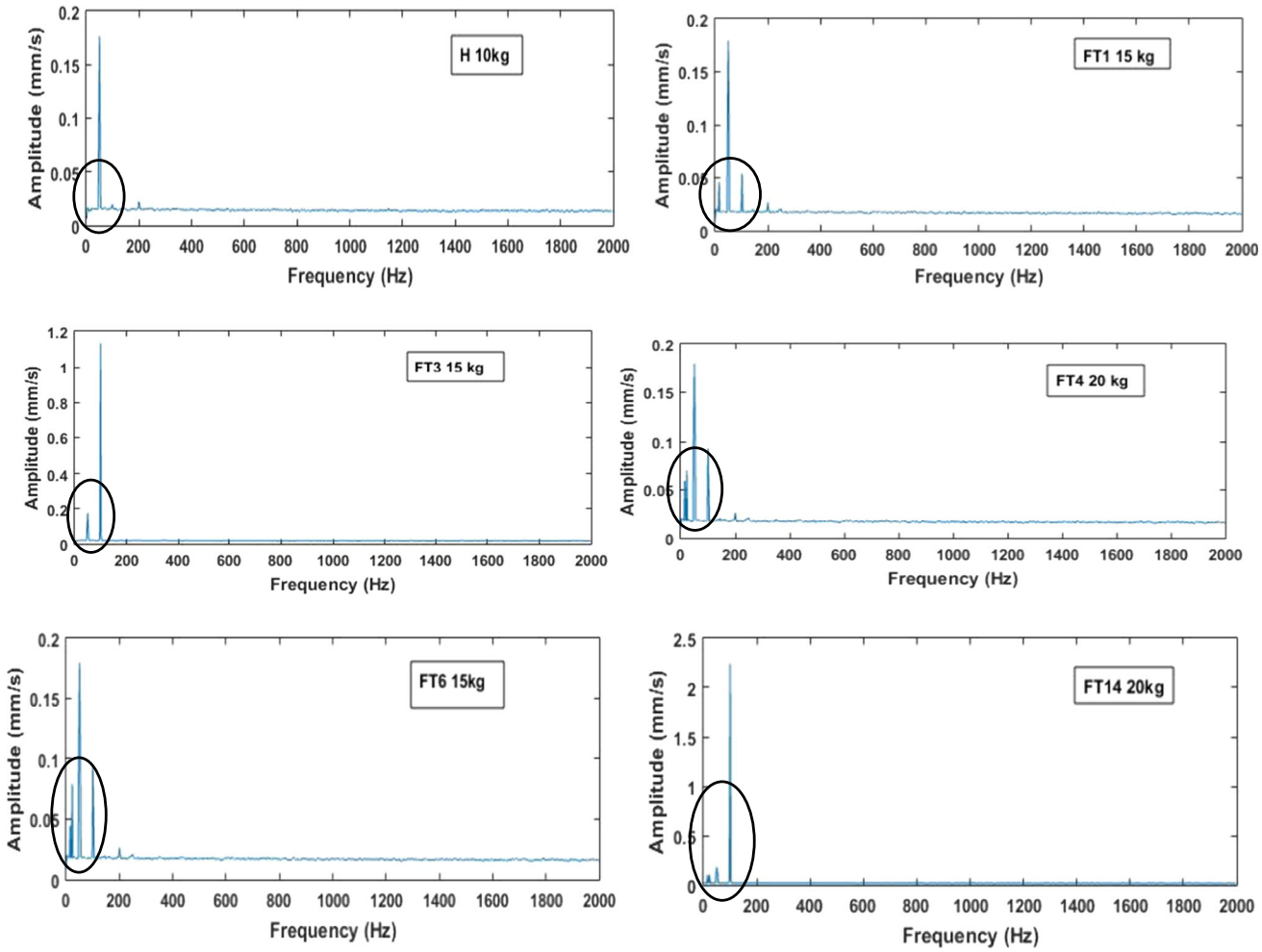

Fig. 6 Denoise vibration signature of healthy, FT2, FT3, FT4, FT6 and FT14 in the frequency domain

I. Orthogonal wavelet transform is used to decompose contaminated vibration signals and to determine required wavelet coefficients. In this step, correct wavelet and wavelet decomposition layers are chosen to determine wavelet coefficients.
II. The convenient threshold is chosen for both layers. Threshold quantization is used to process high-frequency coefficients.
III. The vibration signal is reconstructed by modifying the low-frequency coefficients from the wavelet decomposition layer and high-frequency coefficients from the correct wavelet layer to the wavelet decomposition layer by using inverse wavelet transform.
IV. The above denoising steps are performed in NVGate V10.00 software. NVGate V10.00 software is suitable for the OR34 FFT analyser.

Eight statistical parameters like RMS, crest factor, kurtosis, mean, peak to peak, skewness, sample variance, and standard deviation are extracted from denoised vibration signature in the frequency domain. RMS statistical parameter values are directly given by OR34 FFT analyser NVGate software. The remaining statistical parameters are calculated by the data analysis tool in excel. These parameters are used as input to the train ANN model. ANN model identifies the fault and classifies the fault of the combined worm wheel and bearing.

2.5 ANN model

The ANN model implements the same principle as the human brain applies to find the solution to a complex engineering problem. ANN is based on the existing training algorithm and input–output parameters relationship. Feedforward backpropagation multilayer perceptron ANN is a more popular algorithm than the other available ANN algorithms [16, 19]. Therefore in this research, it is implemented for the classification of faults present in the worm gearbox. Feedforward backpropagation multilayer perceptron (FBMLP) ANN

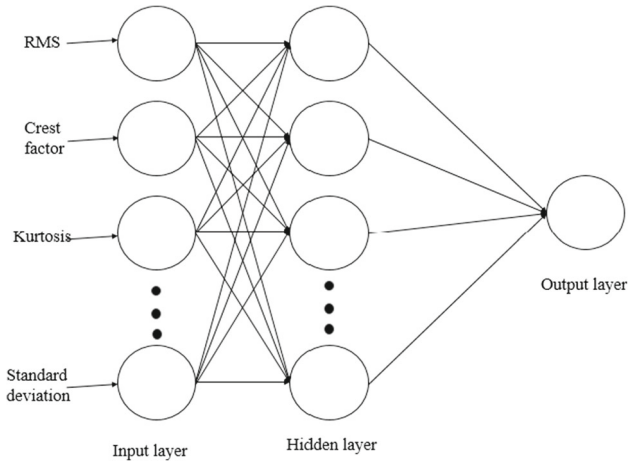

Fig. 7 ANN model

Table 3 Different types of ANN algorithms for fault identification

Number of input neurons	Number of hidden neurons	Number of output neurons	Algorithm
8	8	1	Bayesian algorithm (trainbr)
	10		
	12		
	8		Scaled conjugate gradient algorithm (trainscg)
	10		
	12		
	8		Levenberg-Marquardt algorithm (trainlm)
	10		
	12		

mainly consists of three layers namely, (1) an input layer (2) one hidden layer (3) an output layer as shown in Fig. 7. The input layer has 8 neurons as 8 frequency domain statistical parameters are applied as input to train the ANN model, and the hidden layer neuron is varying from 8 to 12. The output layer has one neuron for fault classification with a 0 or 1 output target value.

From the available literature, in this study, different types of algorithms as mentioned in Table 3 have been implemented to achieve an effective ANN model for current experimentation [19]. MATLAB Neural Network Toolbox is used to train the ANN model. At the beginning of the training of the ANN model, weights and biases are finalized randomly. The total inputs given to the ANN model are 336. ANN model is divided into three sets namely training, testing and validation. Amongst the available data, 70%, 15% and 15% of input data are applied for training, testing, and validation respectively [18]. After testing and validation, it is found that the trainscg algorithm is superior to the trainbr and trainlm algorithms. Therefore ANN mode based on the trainscg algorithm is implemented for the fault identification of the worm gearbox.

3 Results and discussion

3.1 Discussion of experimentation

The vibration amplitudes acquired for the different conditions of the worm gearbox (as shown in Table 2) through the laboratory experimental setup are presented in Table 4. For analysis of FT1, FT2 to FT19; the denoised vibration amplitude of FT1, FT2 to FT19 are compared with a denoise vibration amplitude of healthy worm gearbox at gear mesh frequency of worm wheel (f_{gm}), outer race elements pass frequency (f_{BPOF}), inner race elements pass frequency (f_{BPIF}). These experiments were performed at a load of 10 kg, 15 kg, and 20 kg respectively. In case of a combination of a faulty worm wheel with faulty bearing outer race or faulty bearing inner race; vibration amplitude increases at gear mesh frequency of worm wheel frequency, outer race elements pass frequency (f_{BPOF}) and inner race elements pass frequency (f_{BPIF}) [5, 15, 16]. With the fault present in the worm gearbox, vibration amplitude increases with an increase in load [5]. When a fault is present on the bearing outer race, there is a slight change in the vibration amplitude of the worm wheel at gear mesh frequency. On the other hand, when a fault is present on the bearing inner race, the vibration amplitude of the worm wheel at the gear mesh frequency shows a significant rise. Form result shows that to identify faults present in worm gearbox by using vibration signatures, characteristics rotational frequencies which are gear mesh frequency (f_{gm}), bearing pass outer race frequency (f_{BPOF}), bearing pass Inner race frequency (f_{BPIF}) are strong predictors of worm wheel and bearing faults.

3.2 Discussion on variation of statistical parameters

Variation of statistical parameters for healthy worm gearbox, FT1, FT2 to FT19 is shown in Fig. 8. The values of statistical parameters change with the change in fault location in the worm gearbox [16]. Statistical parameters RMS, mean, peak to peak and standard deviation values for worm wheel, worm wheel bearing inner race and worm wheel bearing outer race increase smoothly with change in a fault condition and load. On the other hand, crest factor, skewness and sample variance value increase and decrease gradually throughout the cycle. In the case of kurtosis; the value up to fault FT6 increased and decreased gradually. While from fault FT7 onwards, the value increases with a smooth trend. Therefore, these parameters

Table 4 Vibration amplitude for the different conditions of worm gearbox

Output speed (r.p.m)	Fault condition	Load (kg)	Denoised vibration signature amplitude at		
			Bearing outer race ($f_{BPOF} = 15.85Hz$)	Bearing inner race ($f_{BPIF} = 22.5Hz$)	Worm wheel ($f_{gm} = 92Hz$)
192	H1	10	0.01524	0.01659	0.0194
	H2	15	0.01594	0.01719	0.02024
	H3	20	0.01675	0.018911	0.02898
	FT1	15	0.046274	0.0178166	0.02183
	FT2	15	0.017316	0.04816	0.05742
	FT3	15	0.01983	0.02161	1.13305
	FT4	10	0.04124	0.05781	0.07924
	FT4	20	0.05924	0.070169	0.092694
	FT5	15	0.054524	0.051659	0.06924
	FT6	15	0.04452	0.07916	0.09394
	FT7	10	0.04324	0.02781	0.9561
	FT7	20	0.04926	0.034023	1.43057
	FT8	15	0.048274	0.04023	2.063057
	FT9	15	0.063481	0.04023	1.43057
	FT10	10	0.01731	0.06317	1.24742
	FT10	20	0.02573	0.074631	1.72474
	FT11	15	0.031731	0.06927	2.12474
	FT12	15	0.031731	0.076927	1.94247
	FT13	10	0.057173	0.08269	2.6910
	FT13	20	0.07421	0.09826	2.8891
	FT14	10	0.079173	0.081692	2.016591
	FT14	20	0.09821	0.108217	2.243891
	FT15	15	0.087108	0.09027	2.128743
	FT15	15	0.087108	0.09027	2.128743
	FT15	15	0.087108	0.09027	2.128743
	FT16	15	0.091810	0.099272	2.798743
	FT17	10	0.06018	0.1038	2.1926
	FT17	20	0.07521	0.1352	2.5926
	FT18	15	0.06298	0.1487	2.858126
	FT19	15	0.0932	0.130187	2.458126

are useful to train the ANN model for fault diagnosis of worm gearbox.

3.3 Discussion of on findings of ANN

In the current research, the train feedforward backpropagation multilayer perceptron ANN model based on trainbr, trainscg and trainlm algorithm is employed to identify various faults that occurred on ribbon blender worm gearbox along with determination of ANN model fault identification accuracy. After testing and validation of the trained ANN model as mentioned in Table 5, it is found that the performance of the trainscg algorithm with 12 hidden neurons is superior to the trainbr and trainlm algorithms [16]. The accuracy of prediction of the ANN model based on the trainscg algorithm with 12 hidden neurons is 95.01%, 99.14% and 99.56% respectively in conjunction with mean square error (MSE) 0.004601 at 29 epochs. Therefore, the ANN model based on the trainscg algorithm is implemented for the identification of worm gearbox condition. To determine the reliability of the proposed ANN model, the trainscg algorithm was trained five times and the confusion matrix was plotted. In this regard, the first trial is considered for the determination of accuracy on training, testing, validation and all confusion matrix. The first trial provides the best validation performance and the confusion matrix is shown in

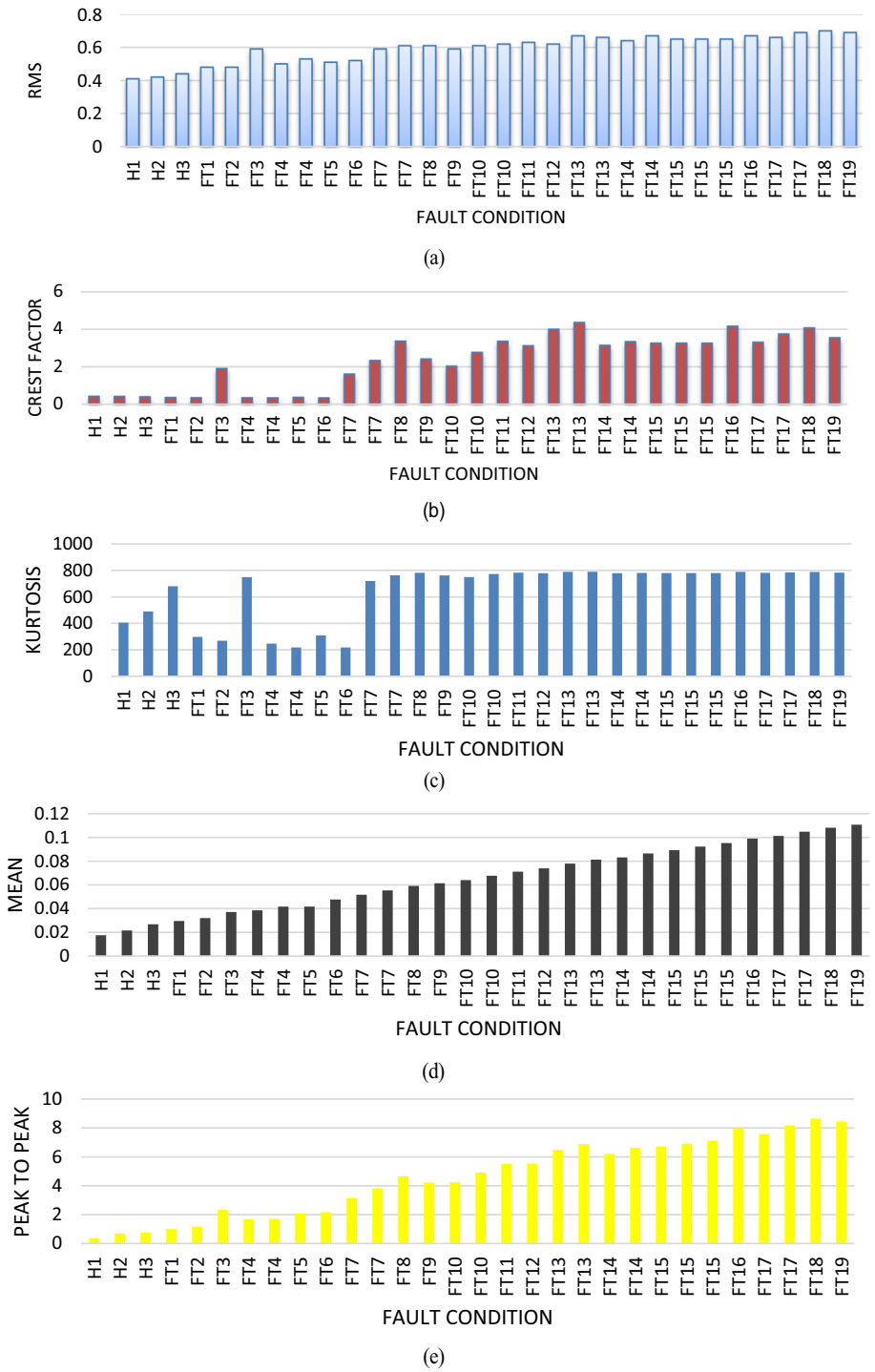

Fig. 8 Frequency domain statistical parameters variation (**a**) RMS (**b**) crest factor (**c**) kurtosis (**d**) mean (**e**) Peak to peak (**f**) skewness (**g**) sample variance (**h**) standard deviation

Fig. 9 and Fig. 10 respectively. Research results show that the trained ANN model identifies healthy conditions (1, 0) and faulty conditions (0, 1) accurately. As proposed ANN model is trained five times, and all confusion matrix fault identification accuracies and cross-entropy are 92.9% each and cross-entropy are 9.2526e-08 (minimum), 6.8131e-07, 2.9473e-07, 1.6454e-07, 2.4948e-07 respectively which differ slightly. Therefore achieved results prove that the ANN model based on the trainscg algorithm with 12 hidden neurons for the first trial. It gives good solidity and reliability to identify worm gearbox faults. Research outcomes envisage that the methodology used in this research has good solidity and effectively improves efficiency, reliability and productivity, lowers the maintenance cost.

Fig. 8 continued

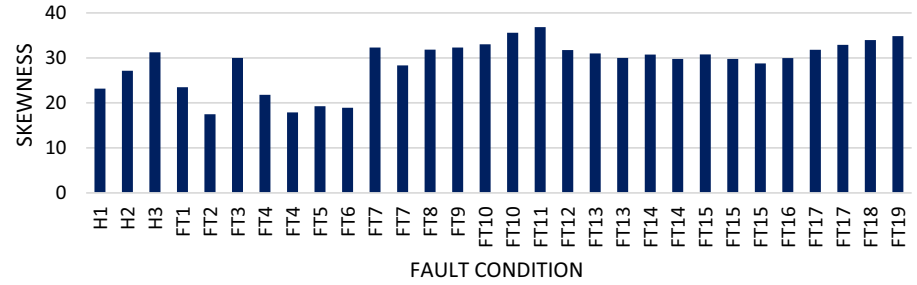

(f)

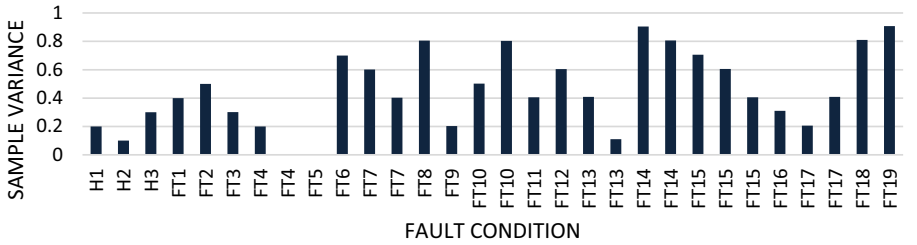

(g)

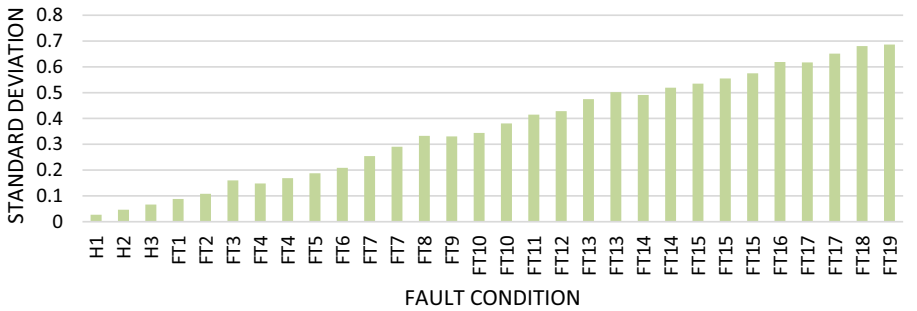

(h)

Table 5 Performance of different types of ANN models for fault identification

Algorithm used	Hidden layer	Epochs	MSE	Accuracy on training data (%)	Accuracy on test data (%)	Accuracy on validation data (%)
trainbr	8	313	4.3233e-12	100	99.9	0
	10	97	5.1476e-12	100	99.98	0
	12	327	4.786e-13	100	99.999	0
trainscg	8	14	0.009175	93.26	98	99.85
	10	23	0.002861	96.41	0	99.22
	12	29	0.004601	95.01	99.14	99.56
trainlm	8	10	9.6726e-05	99.99	0	0
	10	1	0.1498	0	85.67	86.48
	12	3	0.028551	99.35	0	0

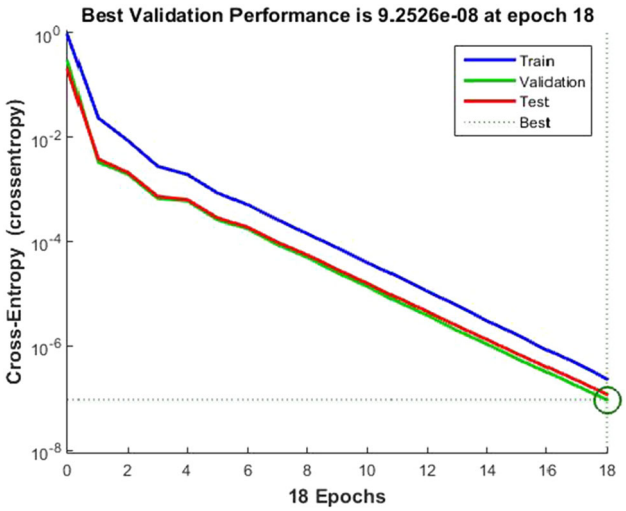

Fig. 9 Best validation performance for the first trial

3.4 Discussion and comparison with previous research work

Table 6 shows that the comparison of present work with previous worm gearbox research work. No work is found reported on the coalesced i.e. combined worm wheel and bearing fault is analysed using vibration monitoring. In this research coalesced fault is analysed by vibration monitoring and the ANN model. Different statistical parameters implemented in previous research which are reported useful for worm wheel and bearing based on time and frequency domain are extracted in the present research work. The Result shows that frequency domain parameters reliably and effectively identify coalesced faults. Umutlu et al. [16] implement an ANN model based on a scaled conjugate gradient algorithm to classify pitting fault severity. The same ANN model and two more ANN models based on the bayesian algorithm and levenberg- marquardt algorithm are implemented to detect worm gearbox conditions. The result proves that the ANN model based on the scaled conjugate gradient algorithm has good prediction potential.

4 Conclusions

In the current research paper, experiments were performed on the worm gearbox by simulating various faults either on the worm wheel or bearing inner and outer race. Further, the combination of faults for two entities and faults on all three entities were examined.

An ANN-based evaluation of the vibration signatures was executed for condition monitoring. The trained model is employed to identify the condition of the worm gearbox. Based on experimentation and the ANN model, subsequent conclusions have been drawn;

1. Laboratory experimental trials show that vibration amplitude varies with changes in the condition of the worm gearbox. When a fault is present on the bearing outer race, there is a slight change in the vibration amplitude of the worm wheel at gear mesh frequency.

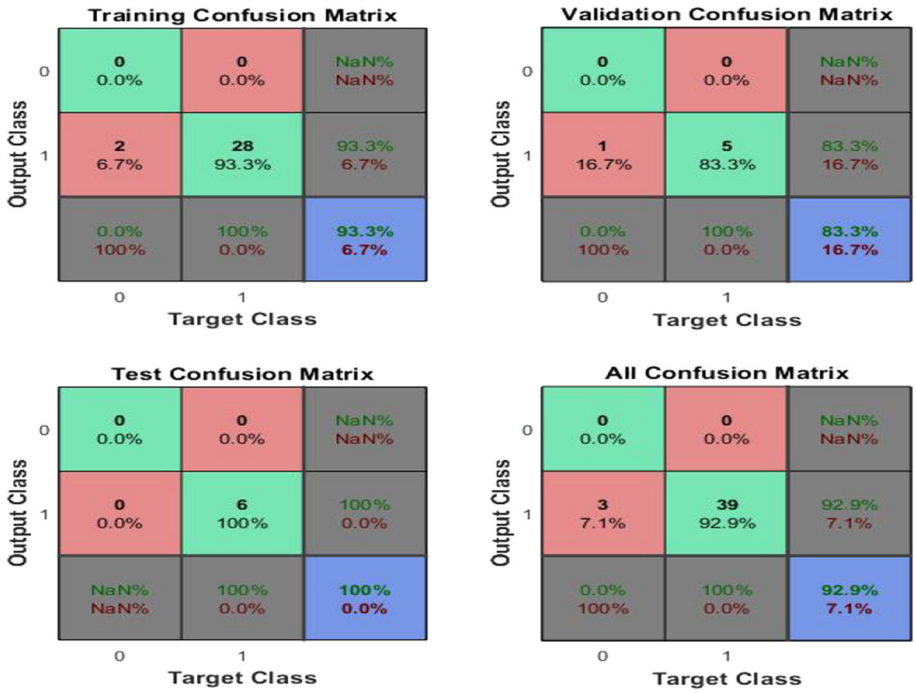

Fig. 10 Confusion matrix for the first trial

Table 6 Comparison of present work with previous worm gearbox research work

Literature	Monitoring techniques	Domain implemented	Extracted statistical parameters	Proposed ANN model	Fault considered	Coalesced fault considered
[13]	Thermal	No	No	No	Single worm wheel tooth breakage	No
[14]	Acoustic emission	Time	RMS, kurtosis	No	Pitting occurred on single worm wheel teeth	No
[15]	Vibration	Time	RMS	No	Worm wheel bearing inner race and outer faulty	No
[16]	Vibration	Time + Frequency	Mean, Median, RMS, standard deviation, peak to peak, crest factor, skewness and kurtosis	Scaled conjugate gradient algorithm	Pitting occurred on multiple worm wheel teeth	No
Present work	Vibration	Frequency	RMS, crest factor, kurtosis, mean, peak to peak, skewness, sample variance, and standard deviation	Bayesian algorithm, Scaled conjugate gradient algorithm and Levenberg-Marquardt algorithm	Nick on bearing inner and outer race, worm wheel tooth breakage and combination all of three	Yes

2. The significant rise in vibration amplitude at the gear mesh frequency is observed when a fault is present on the bearing inner race.
3. Extracted eight statistical parameters like RMS, crest factor, kurtosis, mean, peak to peak, skewness, sample variance and standard deviation varies with the change in fault location in the worm gearbox. Also, the values of statistical features increase with the applied load. Hence, extracted statistical parameters are useful for training the artificial neural network (ANN) models to identify the condition of the worm gearbox.
4. The feedforward backpropagation multilayer perceptron ANN model based on the trainscg algorithm with 12 hidden neurons gives more accuracy for identifying the condition of the worm gearbox than trainbr and trainlm algorithms.
5. Trained ANN model based on trainscg algorithm effectively and reliably classifies various worm gearbox faults such as nick on bearing inner and outer race, worm wheel tooth breakage and combine worm wheel–bearing faulty condition with confusion matrix accuracy of 92.9%.
6. The research outcome envisages that the acquired vibration amplitudes, statistical parameters and ANN model can effectively and reliably monitor the condition of the worm gearbox.

Acknowledgements This work is supported by METs Institute of Engineering management Nashik and, Savitribai Phule Pune University, India.

Author contributions Co-authors contributed equally.

Funding We declare that no funds, grants, or other support were received during the preparation of this manuscript.

Declarations

Conflicts of interest The authors declares no conflict of interest.

References

1. Tang, X., Xu, Y., Sun, X., Liu, Y., Jia, Y., Gu, F., Ball, A.D.: Intelligent fault diagnosis of helical gearboxes with compressive sensing based non-contact measurements. ISA Trans. **20**, 1–16 (2022). https://doi.org/10.1016/j.isatra.2022.07.020
2. Dorantes, J.J.S., Prieto, M.D., Redondo, J.A.O., Rios, R.A.O., Troncoso, R.D.J.R.: Multiple-fault detection methodology based on vibration and current analysis applied to bearings in induction motors and gearboxes on the kinematic chain. Shock. Vib. **2016**, 1–14 (2016). https://doi.org/10.1155/2016/5467643
3. Goyal, D., Choudhary, A., Sandhu, J.K., Srivastava, P., Saxena, K.K.: An intelligent self-adaptive bearing fault diagnosis approach based on improved local mean decomposition. Int. J. Interact. Des. Manuf. (2022). https://doi.org/10.1007/s12008-022-01001-0

4. Maras, S., Arslan, H., Birgoren, B.: Detection of gear wear and faults in spur gear systems using statistical parameters and univariate statistical process control charts. Arab. J. Sci. Eng. **46**, 12221–12234 (2021). https://doi.org/10.1007/s13369-021-05930-y
5. Dhamande, L.S., Chaudhari, M.B.: Compound gear-bearing fault feature extraction using statistical features based on time-frequency method. Measurement **125**, 63–77 (2018). https://doi.org/10.1016/j.measurement.2018.04.059
6. Teng, W., Ding, X., Cheng, H., Han, C., Liu, Y., Mu, H.: Compound faults diagnosis and analysis for a wind turbine gearbox via a novel vibration model and empirical wavelet transform. Renew. Energ. **136**, 393–402 (2019). https://doi.org/10.1016/j.renene.2018.12.094
7. Miao, F., Zhao, R., Wang, X.: A new method of denoising of vibration signal and its application. Shock. Vib. **2**, 1–8 (2020). https://doi.org/10.1155/2020/7587840
8. Miao, F., Zhao, R.: A new fault diagnosis method for rotating machinery based on SCA-FastICA. Shock. Vib. **2**, 1–12 (2020). https://doi.org/10.1155/2020/6576915
9. Xu, A., Huang, W., Li, P., Chen, H., Meng, J., Guo, X.: Mechanical vibration signal denoising using quantum-inspired standard deviation based on subband based gaussian mixture model. Shock. Vib. **2018**, 1–9 (2018). https://doi.org/10.1155/2018/5169070
10. Mishra, C., Samantaray, A.K., Chakraborty, G.: Rolling element bearing fault diagnosis under slow speed operation using wavelet de-noising. Measurement **103**, 77–86 (2017). https://doi.org/10.1016/j.measurement.2017.02.033
11. Karabacak, Y.E., Ozmen, N.G., Gumusel, L.: Worm gear condition monitoring and fault detection from thermal images via deep learning method. Maint. Reliab. **22**, 544–556 (2020). https://doi.org/10.17531/ein.2020.3.18
12. Hizarci, B., Umutlu, R.C., Kiral, Z., Ozturk, H.: Fault severity detection of a worm gearbox based on several feature extraction methods through a developed condition monitoring system. SN Appl. Sci. **3**(1), 129 (2021). https://doi.org/10.1007/s42452-020-04131-w
13. Babu, T.N., Patel, D., Tharnari, D., Bhatt, A.: Temperature behavior-based monitoring of worm gears under different working conditions. Innov. Des. Anal. Dev. Pract. Aerosp. Automot. Eng. **2**, 257–265 (2019). https://doi.org/10.1007/978-981-13-2718-6_24
14. Elforjani, M., Mba, D., Muhammad, A., Sire, A.: Condition monitoring of worm gears. Appl. Acoust. **73**, 859–863 (2012). https://doi.org/10.1016/j.apacoust.2012.03.008
15. Elasha, F., Cárcel, C.R., Mba, D., Kiat, G., Nze, I., Yebra, G.: Pitting detection in worm gearboxes with vibration analysis. Eng. Fail. Anal. **42**, 366–376 (2014). https://doi.org/10.1016/j.engfailanal.2014.04.028
16. Umutlu, R.C., Hizarci, B., Kiral, Z., Ozturk, H.: Classification of pitting fault levels in a worm gearbox using vibration visualization and ANN. Sadhana Acad. Proc. Eng. Sci. **45**, 1–13 (2020). https://doi.org/10.1007/s12046-019-1263
17. Agrawal, P., Jayaswal, P.: Diagnosis and classifications of bearing faults using artificial neural network and support vector machine. J. Inst. Eng. India Ser. C. **101**, 61–72 (2019). https://doi.org/10.1007/s40032-019-00519-9
18. Okwudili, O.E., Ezechukwu, O.A., Onuegbu, J.C.: Artificial neural network method for fault detection on transmission line. Int. J.Eng. Invent. **8**, 47–56 (2019). https://doi.org/10.1109/ICCSCE50387.2020.9204921
19. Kane, P.V., Andhare, A.B.: Critical evaluation and comparison of psychoacoustics, acoustics and vibration features for gear fault correlation and classification. Measurement **154**, 1–28 (2020). https://doi.org/10.1016/j.measurement.2020.107495
20. Dabrowski, D.: Condition monitoring of planetary gearbox by hardware implementation of artificial neural networks. Measurement **91**, 295–308 (2016). https://doi.org/10.1016/j.measurement.2016.05.056
21. Ammar, D.M., Oraby, S.E., Younes, M.A., Elsayed, S.E.: Prediction of bearing service life using an auto regression moving average and response surface methodology. Appl. Model. Simul. **6**, 1–9 (2022)
22. Attoui, I., Fergani, N., Boutasseta, N., Oudjani, B., Deliou, A.: A new time–frequency method for identification and classification of ball bearing faults. J. Sound Vib. **397**, 241–265 (2017). https://doi.org/10.1016/j.jsv.2017.02.041
23. Mishra, H.P., Jalan, A.: Analysis of faults in rotor-bearing system using three-level full factorial design and response surface methodology. Noise Vib. Worldw. **52**, 1–12 (2021). https://doi.org/10.1177/09574565211030711
24. Vanraj, D.S.S., Pabla, B.S.: Optimization of sound sensor placement for condition monitoring of fixed-axis gearbox. Cogent Phys. (2017). https://doi.org/10.1080/23311916.2017.1345673
25. Goyal, D.V., Pabla, B.S., Dhami, S.S.: Non-contact sensor placement strategy for condition monitoring of rotating machine-elements. Eng. Sci. Technol. Int. J. **22**, 489–501 (2019). https://doi.org/10.1016/j.jestch.2018.12.006